Pergamon

Geochimica et Cosmochimica Acta, Vol. 60, No. 6, pp. 1005–1018, 1996

0016-7037/96 $15.00 + .00

PII S0016-7037(96)00011-7

Fractionation of soil gases by diffusion of water vapor, gravitational settling, and thermal diffusion

JEFFREY P. SEVERINGHAUS,[1] MICHAEL L. BENDER,[1] RALPH F. KEELING,[2] and WALLACE S. BROECKER[3]

[1]Graduate School of Oceanography, University of Rhode Island, RI 02881, USA
[2]Scripps Institution of Oceanography, La Jolla, CA 92093, USA
[3]Lamont-Doherty Earth Observatory, Palisades, NY 10964, USA

(*Received March* 7, 1995; *accepted in revised form December* 15, 1995)

Abstract—Air sampled from the moist unsaturated zone in a sand dune exhibits depletion in the heavy isotopes of N_2 and O_2. We propose that the depletion is caused by a diffusive flux of water vapor out of the dune, which sweeps out the other gases, forcing them to diffuse back into the dune. The heavy isotopes of N_2 and O_2 diffuse back more slowly, resulting in a steady-state depletion of the heavy isotopes in the dune interior. We predict the effect's magnitude with molecular diffusion theory and reproduce it in a laboratory simulation, finding good agreement between field, theory, and lab. The magnitude of the effect is governed by the ratio of the binary diffusivities against water vapor of a pair of gases, and increases ~linearly with the difference between the water vapor mole fraction of the site and the advectively mixed reservoir with which it is in diffusive contact (in most cases the atmosphere). The steady-state effect is given by

$$\delta_i = \left[\frac{i/j}{i_o/j_o} - 1\right] 10^3‰ \cong \left[\left(\frac{1 - x_{H_2O}}{1 - x_{H_2O_0}}\right)^{(D_{j-H_2O}/D_{i-H_2O})-1} - 1\right] 10^3‰,$$

where δ_i is the fractional deviation in permil of the gas i/gas j ratio from the advectively mixed reservoir, x_{H_2O} and $x_{H_2O_0}$ are respectively the mole fractions of water vapor at the site and in the advectively mixed reservoir, and D_{i-H_2O} is the binary diffusion coefficient of gas i with water vapor. The effect is independent of scale at steady state, but approaches steady state with the time constant of diffusion set by the length scale. Exploiting the mechanism, we make an experimental estimate of the relative diffusivities of O_2 and N_2 against water vapor, finding that O_2 diffuses 3.6 ± 0.3% faster than N_2 despite its greater mass. We also confirm in the study dune the presence of two additional known processes: gravitational fractionation, heretofore seen only in the unconsolidated firn of polar ice sheets, and thermal diffusion, well described in laboratory studies but not seen previously in nature. We predict that soil gases in general will exhibit the three effects described here, the water vapor flux fractionation effect, gravitational fractionation, and thermal diffusion. However, our analysis neglects Knudsen diffusion and thus may be inapplicable to fine-grained soils.

1. INTRODUCTION

Gases and their isotopes dissolved in groundwater have found a variety of environmental and hydrologic applications. For example, noble gas abundances in groundwater recharged during the last glacial maximum have been used to infer paleotemperature during the glacial epoch (Stute et al., 1992; Mazor, 1972). Because the composition of the gas in the unsaturated zone of the recharge area sets the composition of the dissolved gases in groundwater, processes governing unsaturated zone gas composition must be considered by these studies. We report here on one such process, which to the best of our knowledge has not previously been described. We also report on two additional processes, thermal diffusion and gravitational settling, that we believe have not previously been noted in soil gases.

While studying the feasibility of using the gases in the vadose zone of sand dunes to reconstruct decadal changes in atmospheric composition (Severinghaus, 1995), we observed an anomaly in the isotopic composition of molecular nitrogen (N_2) and oxygen (O_2) in vadose air from a sand dune. The heavy isotopic species $^{15}N^{14}N$ and $^{18}O^{16}O$ were depleted relative to the free atmosphere by up to −0.2 and −0.4‰ respectively, in the customary δ units:

$$\delta^{15}N = [(^{15}N/^{14}N_{sample})/(^{15}N/^{14}N_{free\ air}) - 1] \times 10^3‰. \quad (1)$$

This observation ran contrary to our expectation that the heavier gas species in deep unsaturated zones of soils would be enriched by gravitational settling (Gibbs, 1928), as is observed in gases in the deep layer of unconsolidated snow on top of polar ice sheets (Craig et al., 1988; Sowers et al., 1989; Schwander et al., 1993; Bender et al., 1994a).

It is easily shown that the anomaly cannot be due to biological activity: if addition of biogenic N_2 with $\delta^{15}N = -30‰$ (an extreme value; Delwiche and Steyn, 1970) were the cause, then the Ar/N_2 ratio would have dropped by 7‰ assuming that argon is conserved. In fact, the Ar/N_2 ratio (measured mass spectrometrically) was unchanged within the analytical uncertainty of 1‰. Likewise, fractionation during respiratory consumption of O_2 cannot explain the ^{18}O anomaly, since respiration consumes the light isotope

preferentially (Schleser, 1979), leaving the remaining gas enriched in ^{18}O and thus producing an effect of the wrong sign.

In this paper we propose the hypothesis that the anomaly is due to diffusion of water vapor out of the moist interior of the dune into the dry desert air. The physical basis for this mechanism is that the binary diffusion coefficient of a given gas into H_2O vapor is smaller for a heavier isotopic species (such as $^{15}N^{14}N$) than for a light isotopic species (such as $^{14}N_2$). Diffusive transport is a mutual phenomenon; a gas must diffuse against another gas (Bird et al., 1960). In this case H_2O vapor and N_2 (for example) mutually diffuse against one another. The familiar relation

$$J = -D\nabla C, \tag{2}$$

where J is the diffusive flux, D is the binary diffusion coefficient, and ∇C is the concentration gradient, is valid only in the reference frame in which there is no net flow of gas (Reid et al., 1977). Because there is a net flux of water vapor out of the dune, this reference frame moves upward with respect to the dune. In other words, in this reference frame, N_2 is diffusing downwards. The heavier N_2 species will diffuse more slowly than the light N_2 species, leading to a steady-state depletion of the heavier isotopes in the air.

An alternative, perhaps more intuitive, way to understand the mechanism is that the mole fraction of H_2O vapor is about 3% in saturated air at 25°C, the conditions obtaining in the interior of the dune. In the dry desert air above the dune, the mole fraction of H_2O vapor is nearly zero. Therefore, the mole fraction of N_2 will be only ~75% in the dune but 78% in the free air. This gradient will drive a diffusive flux of N_2 into the dune, which must be matched by an advective flux out of the dune, since there can be no net flux of N_2 as there are no N_2 sources or sinks. The light isotopic species will diffuse faster into the dune than the heavy isotopic species, while all species are advected equally out of the dune, leading to a steady state enrichment of the light isotopic species in the dune interior.

We test the hypothesis in two independent ways: with molecular diffusion theory and a laboratory simulation of the effect. The two approaches give good agreement with each other and with the observed anomaly in the dunes. We show that the effect is true for molecular pairs of gases in general as well as isotopic species, and predict that the effect will occur in any situation in which a gradient of water vapor mole fraction exists in a diffusive medium. We go on to examine the implications of this effect for noble gas ratios in deep unsaturated zones, and leaf stomatal fractionation of the isotopes of CO_2. Because water vapor gradients are ubiquitous on Earth, this effect will occur commonly enough to warrant having a simple name. We call it the water vapor flux fractionation effect.

1.1. Expected Isotopic Composition of Soil Gas Based on Known Processes

1.1.1. Gravitational fractionation

The increase of partial pressure of a gas toward the bottom of a column of air in a gravitational field is given by the barometric equation, provided that vertical transport is primarily by diffusion (Dalton, 1826; Gibbs, 1928; Craig et al., 1988):

$$P = P_o \exp[mgz/R^*T], \tag{3}$$

where P = partial pressure of a gas, P_o = surface partial pressure of that gas, m = molecular mass, g = acceleration of gravity, z = depth below surface, R^* = gas constant, and T = temperature in K. The enrichment of a heavy gas species relative to a light species is derived from Eqn. 3 and is given by (Craig et al., 1988):

$$\delta = [R/R_o - 1]10^3‰$$
$$= [\exp(\Delta mgz/R^*T) - 1]10^3‰, \tag{4}$$

where δ = the fractional deviation of a gas pair ratio R from a reference ratio R_o and Δm = the mass difference between the two species. We expect gravitational equilibrium in the dune studied here because analyses of chlorofluorocarbon concentration and ^{85}Kr activity strongly argue that diffusion is the dominant transport process in this dune (Severinghaus, 1995). While barometric pressure changes and wind-induced "pumping" surely cause some advective flow in soils (Weeks, 1994; Clements and Wilkening, 1974), gas diffusivities in soils with high gas-phase porosities are of the order of 1 m^2 per day (Hesterberg and Siegenthaler, 1991), so it is perhaps not surprising that diffusion dominates advection as a transport mechanism here.

1.1.2. Thermal diffusion

Gas mixtures in the presence of a temperature gradient will become fractionated due to a process known as thermal diffusion, provided again that transport is primarily by diffusion (Chapman and Dootson, 1917; Grew and Ibbs, 1952; Chapman and Cowling, 1970; Kincaid et al., 1987). Generally, the species with greater mass will migrate towards the cold end of the temperature gradient, though molecular size, temperature, and mixture composition also play a role (Kincaid et al., 1987). As concentration gradients develop in the mixture a steady state is reached in which the flux due to thermal diffusion in one direction is balanced by a flux driven by concentration diffusion in the other direction. In this situation the magnitude of the effect is given by (Chapman and Cowling, 1970):

$$\delta = [R/R_o - 1]10^3‰ = ([T_o/T]^\alpha - 1)10^3‰, \tag{5}$$

where δ is the fractional deviation of a gas pair ratio R from a reference ratio R_o, T is temperature in K and T_o is the temperature of R_o, and α is the thermal diffusion factor (Grew and Ibbs, 1952), an experimental constant characteristic of a pair of gas species. For example, α for the isotopic pair $^{15}N^{14}N$-$^{14}N_2$ is about 0.0065 at 298 K (Grew and Ibbs, 1952), so a temperature gradient between 298 and 308 K will cause the warm end to have $\delta^{15}N = -0.2‰$ relative to the cold end.

2. OBSERVATIONS: ANOMALY IN SAND DUNES

We sampled air from dunes in the Algodones dune field located along the eastern margin of the Imperial Valley of California, USA,

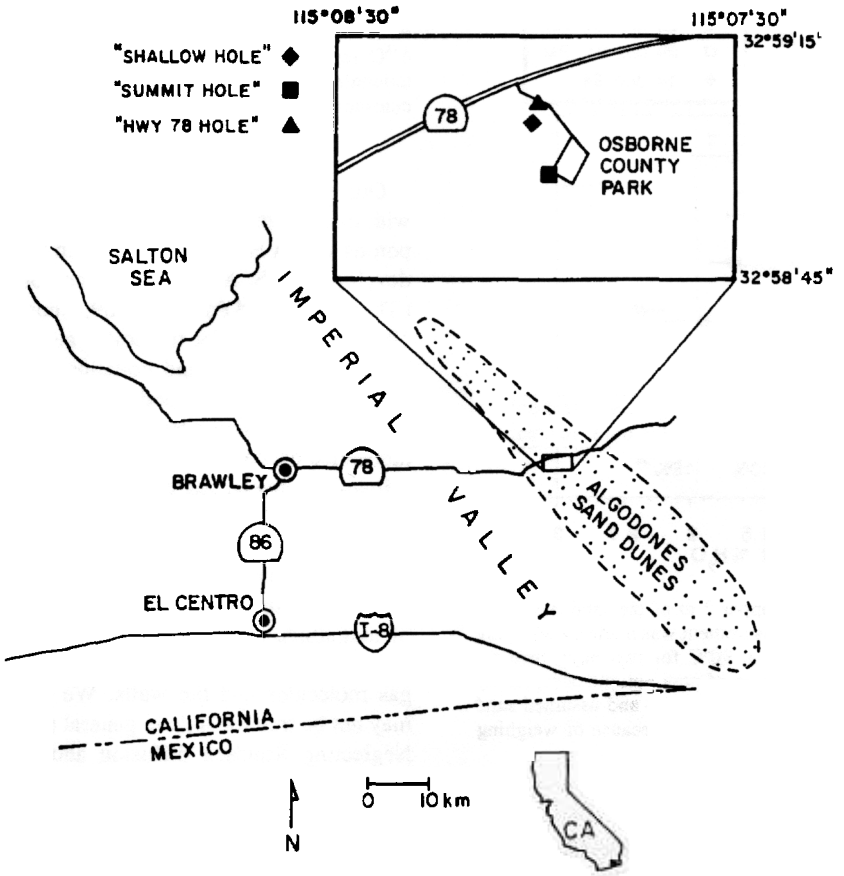

FIG. 1. Location of the study area. Inset shows locations of the three holes drilled, named "Hwy 78" (60 m deep), "Summit" (60 m deep), and "Shallow" (8 m deep). The site was chosen for logistical reasons, being the only place in North America where a paved road goes to the top of a major sand dune.

near the Mexican border (32°59'N, 115°08'W; Fig. 1). Mean annual precipitation at the site is ~50 mm y^{-1} (Sweet et al., 1991), and mean annual soil temperature at the surface is 25.8°C based on our measurements. The unsaturated zone is about 100 m thick at the site, based on the elevation of the water table in wells 5 km east and west of the site (USGS, 1976). Dune migration is less than 0.25 m y^{-1} (Sweet et al., 1991), compared with effective gas diffusivities of ~1 m^2 d^{-1} (a typical value for soil; Hesterberg and Siegenthaler, 1991), meaning that dune migration is not an issue in terms of the exchange of the soil air with the atmosphere.

Despite the aridity and the deep water table, the sand is wet (that is, liquid water coats the grains) at depths of as little as 20 cm (Fig. 2). This is not so surprising when one considers that sand has little capillarity because of the relatively large smooth grains. Thus, to escape upward from the dune, moisture must traverse a dry sand zone in the gas phase. With diffusivities on the order of ~1 m^2 d^{-1}, a dry sand layer 0.5 m thick, a porosity of 0.3, and dry atmosphere, only ~5 mm y^{-1} of water would escape to the atmosphere by diffusion, far less than the 50 mm y^{-1} of precipitation. Near-surface advection of air may greatly increase vapor transport, however.

2.1. Sampling Procedure

To extract air from the interior of the dune, we drilled two 60 m deep holes with a hollow stem auger and an 8 m deep hole with a hand auger. To sample a variety of depths we inserted tubing of various lengths with stainless steel screens (100 μm mesh) fixed to the ends of the tubing, and then backfilled the holes with sand. Four-wire thermisters calibrated in the laboratory were inserted along with the tubing in the 60 m deep holes. Sampling was done one to four months later by pumping on the tubes, and storing cryogenically dried sample in 2 L flow-through glass flasks with viton O-rings. Contamination by surface air during the drilling procedure was shown to be negligible by analyses of chlorofluorocarbon concentration (Severinghaus, 1995). To ascertain that our sampling apparatus was not fractionating the samples, we sampled surface air through the complete apparatus with tubing and screen inserted into a bucket of dry sand, and these gave a null result. For a complete description of the sampling procedure and the site characteristics see Severinghaus (1995).

2.2. Isotopic Analysis

Samples from the 60 m holes and the 8 m hole were analyzed at the University of Rhode Island on Finnegan MAT 251 and 252 isotope ratio mass spectrometers, respectively. We measured the mass 29/28 ($^{15}N^{14}N/^{14}N_2$) and mass 34/32 ($^{18}O^{16}O/^{16}O_2$) ratios in whole air. The MAT 251 has a glass inlet line and Louwers-Hapert valves, and operates at an inlet pressure of 1 atm. About 25 cm^3 STP of dry sample is admitted to the inlet line and analyzed against a similar aliquot of a dry air standard. Sample and reference are admitted to the changeover valve through 1 m long, 10 μm i.d. glass capillary tubing. Precision, based on repeated admission of aliquots, was ± 0.005‰ for $\delta^{15}N$ of N_2 and ±0.02‰ for $\delta^{18}O$ of O_2. The samples from the 8 m hole were run on the MAT 252 with a conventional inlet, and precision for these samples is estimated at ±0.02‰ for $\delta^{15}N$ of N_2 and ±0.04‰ for $\delta^{18}O$ of O_2. All reported errors are 1 σ. Atmospheric isotope ratios are used as the standards for N_2 and

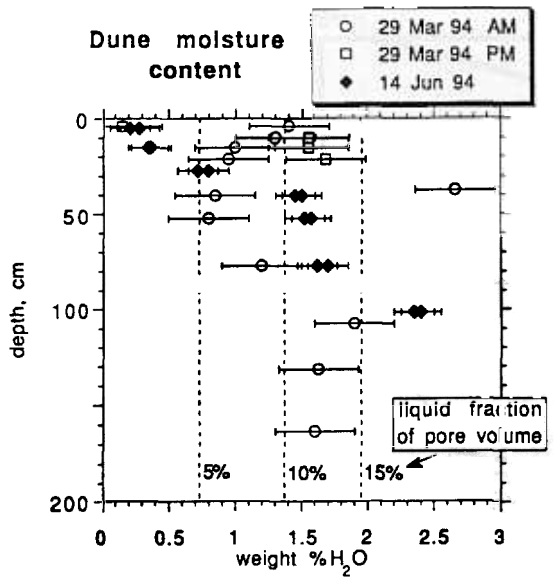

FIG. 2. Moisture content of the upper 2 m of the sand dune near the Shallow hole at three times. Measurement was made by weighing a fresh sample, drying in an oven at 90°C for two days, then reweighing. Dashed lines are the fraction of pore volume occupied by liquid water, calculated from measured porosity and assumed sand grain specific gravity of 2.7. Error bars differ because of weighing balance quality.

O_2 isotopic measurements, as these ratios are constant to a very high level in the free troposphere in comparison to current measurement capability.

The $\delta^{15}N$ data were corrected for isobaric interference at masses 29 and 28 from carbon monoxide ($^{13}CO^+$ and $^{12}CO^+$) produced in the mass spectrometer source from CO_2 present in the sample. Following the procedure outlined by Bender et al. (1994b) we correct the data using the independently measured CO_2 concentrations of the samples (Severinghaus, 1995) according to

$$\delta^{15}N_{actual} = \delta^{15}N_{measured} - 0.000037‰/\text{ppmV } CO_2 \times (CO_{2sample} - CO_{2standard}). \quad (6)$$

As the CO_2 concentrations in the samples ranged up to ~500 ppmV greater than in the standard, the correction ranged up to 0.018‰.

The $\delta^{18}O$ data obtained on the MAT 251 were corrected for the sensitivity of this mass spectrometer to differences in the O_2/N_2 ratios of the sample and standard gases. Following Sowers et al. (1989) we correct by the following:

$$\delta^{18}O_{actual} = \delta^{18}O_{measured} + 0.05 \times \delta N_2/O_2 \text{ (mass 29/mass 32)}. \quad (7)$$

As $\delta N_2/O_2$ was as large as +1.22‰, the correction was as large as 0.06‰.

Several tests were performed to identify sampling artifacts, in which samples were drawn at a range of flow rates from 1 to 5 Lpm, and before and after pumping 1000 L of air. No significant variations were found in $\delta^{15}N$ in these tests ($\delta^{18}O$ was not analyzed), and in Fig. 3 the test results are difficult to see because the points appear on top of each other. The reproducibility of the $\delta^{15}N$ measurement, based on four replicate samples drawn from 52 m depth on the same day, was ±0.004‰ (one standard deviation). However, greater variation is observed between samples taken two months apart, so the error of our estimate of the dune air's true composition is conservatively ±0.02‰ for $\delta^{15}N$. Repeat measurements of $\delta^{18}O$ were not made, but our guess is that the corresponding error is ±0.05‰.

Figure 3 and Table 1 show the results of all samples taken from the three holes. As seen in Fig. 3, the depletions are still much larger than these errors, amounting to about −0.2 and −0.4‰ below the value expected for gravitational/thermal equilibrium for $\delta^{15}N$ and $\delta^{18}O$, respectively. Despite the depletion, however, the correct gravitational/thermal slope is apparent in both gases, with a more or less constant offset.

3. MOLECULAR DIFFUSION THEORY

Our hypothesis to explain these anomalous data is testable with existing theories of gaseous diffusion. Gas transport in porous media is often treated with the "dusty gas" model developed by E. A. Mason and coworkers in the late 1960s (Thorstenson and Pollock, 1989; Cunningham and Williams, 1980). In this model the soil grains are treated essentially as giant molecules, and collisions between gas molecules and soil grains are treated with a Knudsen diffusion term. (Knudsen diffusion occurs when the mean free path of the molecules exceeds the pore diameter, so that collisions are primarily between gas molecules and the walls; Bird et al., 1960.)

In the present study we neglect the effects of Knudsen diffusion, because the mean free path is of the order of 1 μm whereas the sand dune pore sizes are two to three orders of magnitude larger. Thus, in the dune, collisions between gas molecules are far more common than collisions between gas molecules and the walls. We note, however, that this may not be true for soils in general (e.g., fine-grained soils). Neglecting Knudsen diffusion and other wall effects, the dusty gas model simplifies to the equations for multicomponent diffusion in a system without walls, known as the Stefan-Maxwell equations (Thorstenson and Pollock, 1989), which we employ here.

Figure 4 diagrams the proposed mechanism in an idealized case with only three gas species: i = rare isotopic species (e.g., $^{15}N^{14}N$); j = abundant isotopic species (e.g., $^{14}N_2$); and H_2O vapor. In this steady state idealized case, a diffusive region of constant tortuosity with a constant upward flux of water vapor supports a nearly linear gradient in H_2O vapor mole fraction between the wetting front, where liquid water coats the sand grains, and the atmosphere, an advectively well-stirred region maintained at low humidity. (We neglect a slight deviation from linearity that occurs due to the fact that the contribution to the total water vapor flux arising from "advection" decreases as the mole fraction of water vapor decreases, causing the gradient to steepen as the vapor mole fraction decreases; see Bird et al., 1960, page 523.)

The relative humidity at the wetting front is assumed to be 100%, since the resaturation time of the pore gas is likely to be fast relative to the residence time of vapor in the pore. The gradient in H_2O vapor results in a reverse gradient in all other gases, henceforth known as the "stagnant gases" (for example, N_2). In the no-net-flow reference frame in which the diffusion equation is valid, as previously discussed, this reverse gradient drives a diffusive flux of the stagnant gases downward, while the reference frame itself moves upward with respect to the dune, resulting in no net flow of the stagnant gases with respect to the dune as required. We note that the advective flux caused by upward movement of the reference frame is equivalent to the "nonequimolar flux" of Cunningham and Williams (1980) and Thorstenson and Pollock (1989).

Table 1. Isotopic analyses of N2 and O2 in sand dune

Date sampled	Hole	Depth, m	Flask ID	Raw data* d15N	Raw data* d18O	Corrected for CO isobaric interference d15N	Corrected for sensitivity to O2/N2 d18O
4-Jan-94	Hwy 78	12.20	401	-0.140	-0.324	-0.158	-0.263
4-Jan-94	Hwy 78	24.39	403	-0.104	-0.201	-0.118	-0.149
4-Jan-94	Hwy 78	33.54	402	-0.102	-0.191	-0.115	-0.148
4-Jan-94	Hwy 78	42.68	404	-0.097	-0.163	-0.109	-0.133
4-Jan-94	Hwy 78	51.83	405	-0.082	-0.066	-0.093	-0.047
4-Jan-94	Hwy 78	60.98	406	-0.065	-0.019	-0.080	0.006
4-Jan-94	Summit	39.63	407	-0.072	-0.044	-0.081	-0.062
4-Jan-94	Summit	54.88	408	-0.065	-0.036	-0.075	-0.076
28-Feb-94	Hwy 78	-1.00	103	0.013	not	0.000	
28-Feb-94	Hwy 78	12.20	100	-0.186	measured	-0.217	
28-Feb-94	Hwy 78	12.20	111	-0.187		-0.218	
28-Feb-94	Hwy 78	24.39	109	-0.111		-0.138	
28-Feb-94	Hwy 78	33.54	110	-0.096		-0.122	
28-Feb-94	Hwy 78	42.68	108	-0.087		-0.112	
28-Feb-94	Hwy 78	51.83	403	-0.077		-0.102	
28-Feb-94	Hwy 78	51.83	404	-0.075		-0.100	
28-Feb-94	Hwy 78	51.83	405	-0.079		-0.104	
28-Feb-94	Hwy 78	51.83	406	-0.069		-0.094	
28-Feb-94	Hwy 78	60.98	401	-0.076		-0.104	
28-Feb-94	Hwy 78	60.98	402	-0.076		-0.102	
28-Mar-94	Shallow	0.91	112	-0.015	-0.023	-0.016	-0.023
28-Mar-94	Shallow	1.52	113	-0.108	-0.202	-0.110	-0.202
28-Mar-94	Shallow	2.74	114	-0.086	-0.206	-0.089	-0.206
28-Mar-94	Shallow	4.57	115	-0.108	-0.195	-0.112	-0.195
28-Mar-94	Shallow	6.10	104	-0.161	-0.267	-0.171	-0.267
28-Mar-94	Shallow	8.08	105	-0.191	-0.286	-0.204	-0.286
29-Mar-94	Summit	9.15	106	-0.220	-0.361	-0.234	-0.361
29-Mar-94	Summit	23.35	107	-0.111	-0.138	-0.120	-0.138
4-Sep-94	Shallow	-1	405	-0.005	0.007	0.000	0.003
4-Sep-94	Shallow	1.96	100	-0.191	-0.324	-0.188	-0.356
4-Sep-94	Shallow	3.02	112	-0.109	-0.218	-0.108	-0.229
4-Sep-94	Shallow	4.22	113	-0.046	-0.128	-0.045	-0.118
4-Sep-94	Shallow	5.51	114	0.005	-0.057	0.003	-0.035
4-Sep-94	Shallow	6.91	115	0.006	-0.078	0.000	-0.046
4-Sep-94	Summit	9.15	104	0.017	-0.025	0.008	0.012
4-Sep-94	Summit	23.35	106	-0.120	-0.186	-0.124	-0.189

*corrected for zero enrichment

Assuming as is normally done that diffusivities of gas species are independent of composition, the Stefan-Maxwell equations with three gases are (Reid et al., 1977)

$$\frac{dx_i}{dz} = \frac{x_i x_j}{D_{i-j}}\left[\frac{J_j}{c_j} - \frac{J_i}{c_i}\right] + \frac{x_i x_{H_2O}}{D_{i-H_2O}}\left[\frac{J_{H_2O}}{c_{H_2O}} - \frac{J_i}{c_i}\right], \quad (8)$$

$$\frac{dx_j}{dz} = \frac{x_j x_i}{D_{j-i}}\left[\frac{J_i}{c_i} - \frac{J_j}{c_j}\right] + \frac{x_j x_{H_2O}}{D_{j-H_2O}}\left[\frac{J_{H_2O}}{c_{H_2O}} - \frac{J_j}{c_j}\right], \quad (9)$$

where x = mole fraction, z = depth, D_{i-j} = binary diffusion coefficient of gas i into gas j, c = concentration, J = diffusive flux in the no-net-flow reference frame, u = velocity of the no-net-flow reference frame with respect to the dune, and ϕ = porosity. Some simplification is possible, by taking advantage of the constraint that no net flow of stagnant gases occur with respect to the dune at steady state. The downward diffusive flux of gas i or j must be balanced by the upward flux due to movement of the no-net-flux reference frame with respect to the dune:

$$\text{so} \qquad J_i + uc_i\phi = 0 = J_j + uc_j\phi, \quad (10)$$

where $uc\phi$ = flux arising from the movement of the no-net-flux reference frame. Because the velocity u is the same for all species, Eqn. 10 simplifies to

$$\frac{J_i}{c_i} = \frac{J_j}{c_j}. \quad (11)$$

In words, the diffusion velocity of all stagnant gases must be equal at steady state. Therefore, the first terms on the right-hand side of Eqns. 8 and 9 are zero. This implies that

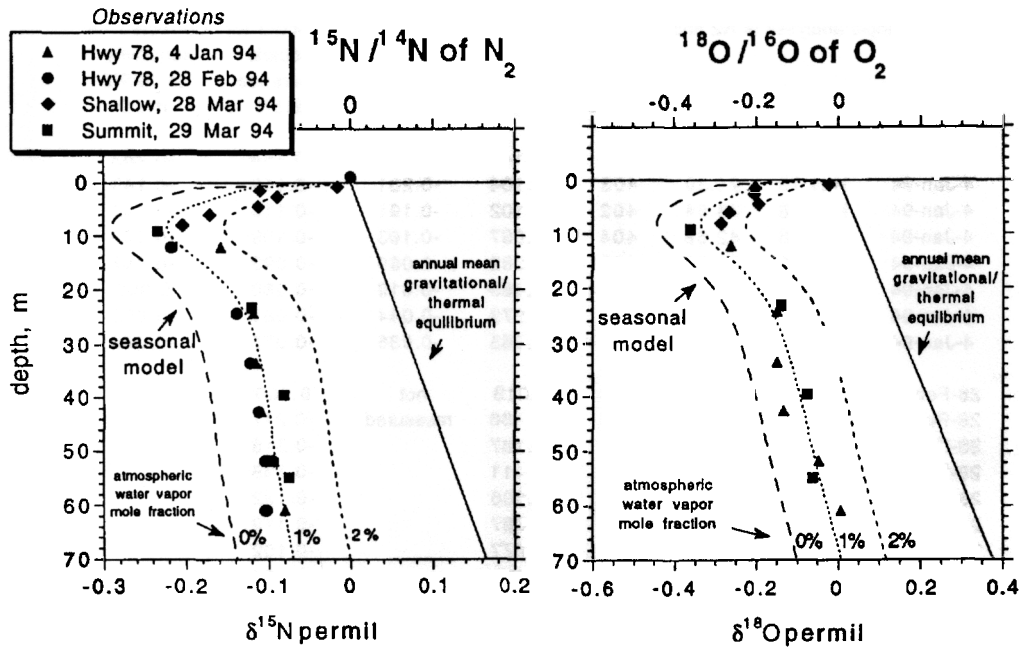

FIG. 3. Depth profiles of the isotopes of air withdrawn from the study sand dune. Note that $\delta^{15}N$ is offset about 0.2‰ from the expected gravitational/thermal equilibrium profile, and $\delta^{18}O$ is offset roughly twice that amount, suggesting a mass-dependent fractionation. The dashed lines are model profiles predicted by the hypothesis of this paper, that the offset is due to a diffusive flux of water vapor out of the dune into the dry desert air, modulated by gravity and thermal effects. Model day is March 28. Although the atmospheric vapor mole fraction is not well known, and thus represents a free parameter in the model, the model clearly reproduces the slope and shape of the data. For both ^{15}N and ^{18}O the model fits a plausible atmospheric vapor mole fraction of 1% (see text).

we can add any number of other stagnant gases to our idealized three-gas system, and the Stefan-Maxwell equations still simplify to

$$\frac{dx_i}{dz} = \frac{x_i x_{H_2O}}{D_{i-H_2O}}\left[\frac{J_{H_2O}}{c_{H_2O}} - \frac{J_i}{c_i}\right], \tag{12}$$

$$\frac{dx_j}{dz} = \frac{x_j x_{H_2O}}{D_{j-H_2O}}\left[\frac{J_{H_2O}}{c_{H_2O}} - \frac{J_j}{c_j}\right]. \tag{13}$$

Dividing Eqn. 12 by 13 and noting that, because of Eqn. 11, the term in brackets in Eqn. 12 equals the term in brackets in Eqn. 13, we obtain

$$\frac{dx_i}{dx_j} = \frac{x_i D_{j-H_2O}}{x_j D_{i-H_2O}}$$

or

$$\int_{x_{io}}^{x_i} \frac{dx_i}{x_i} = \frac{D_{j-H_2O}}{D_{i-H_2O}} \int_{x_{jo}}^{x_j} \frac{dx_j}{x_j},$$

where x_o is the atmospheric mole fraction and serves as a boundary condition, giving

$$\frac{x_i}{x_{io}} = \left(\frac{x_j}{x_{jo}}\right)^{(D_{j-H_2O}/D_{i-H_2O})} \tag{16}$$

and finally, converting to the geochemist's delta notation:

$$\delta_i = \left[\left(\frac{x_j}{x_{jo}}\right)^{(D_{j-H_2O}/D_{i-H_2O})-1} - 1\right] 10^3‰. \tag{17}$$

Equation 17 gives the magnitude of the effect exactly. Note that it is a simple function of the reduction in mole fraction of gas j and of the ratio of the diffusivities of the two gases against water. There is no scale dependence, nor is there any explicit mass dependence, so the effect should be true for molecular pairs, for example, the ratio Xe/N_2, as well as isotopes. Ideally we would like to express Eqn. 17 in a form independent of the (unknown) variable x_j. Exploiting the fact that

$$x_i + x_j + x_{H_2O} + x_k = 1, \tag{18}$$

where x_k is the mole fraction of all other gas species present, and

$$x_{io} + x_{jo} + x_{H_2O_0} + x_{ko} = 1, \tag{19}$$

where $x_{H_2O_0}$ is the atmospheric water vapor mole fraction, Eqn. 17 may be written as

$$\delta_i = \left[\left(\frac{1 - x_{H_2O} - x_k}{\dfrac{x_{io}\delta_i 10^{-3} + 1 - x_{H_2O_0} - x_{k_o}}{}}\right)^{(D_{j-H_2O}/D_{i-H_2O})-1} - 1\right]$$

The term $x_{io}\delta_i 10^{-3}$ is of order 10^{-6} and may be neglected.

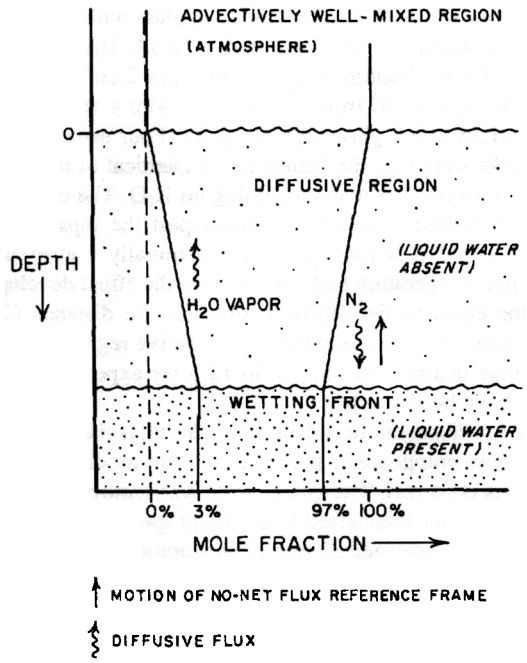

FIG. 4. Schematic diagram of the proposed mechanism. A gradient of water vapor drives a diffusive flux upward, and the complementary gradient in N_2 drives a diffusive flux downward, causing isotopic fractionation of the isotopes of N_2. A velocity u of the no-net-flux reference frame is required to balance the N_2 flux into the dune. In the real dune the depth to the wetting front was 10–20 cm in March and June 1994 (Fig. 2).

Because

$$\frac{x_k}{x_{ko}} \approx \frac{(1 - X_{H_2O})}{(1 - X_{H_2O_0})}, \tag{21}$$

we may drop the terms X_k and X_{ko} from Eqn. 20 with an error of about 0.001‰ in δ_i. These approximations result in the final equation describing the effect

$$\delta_i = \left[\frac{i/j}{i_o/j_o} - 1\right] 10^3‰$$

$$\cong \left[\left(\frac{1 - x_{H_2O}}{1 - x_{H_2O_0}}\right)^{(D_{j-H_2O}/D_{i-H_2O})-1} - 1\right]$$

A useful shorthand version of Eqn. 22, good to a few parts in 10^3, is

$$\delta_i \approx -\Delta x_{H_2O}\left(\frac{D_{j-H_2O}}{D_{i-H_2O}} - 1\right) 10^3‰, \tag{23}$$

where ΔX_{H_2O} is the difference in water vapor mole fraction between the site of interest and the advectively mixed region. The diffusivity ratio for isotopic pairs is a function of the molecular masses m only (Reid et al., 1977):

$$\frac{D_{j-H_2O}}{D_{i-H_2O}} = \left[\frac{\dfrac{m_j + m_{H_2O}}{m_j m_{H_2O}}}{\dfrac{m_i + m_{H_2O}}{m_i m_{H_2O}}}\right]^{1/2} \tag{24}$$

For example, the isotopes of N_2 give

$$\frac{D_{N14-H_2O}}{D_{N15-H_2O}} = \left[\frac{\dfrac{28 + 18}{28 \times 18}}{\dfrac{29 + 18}{29 \times 18}}\right]^{1/2} = 1.0068. \tag{25}$$

At 25°C, 1 atm, and 100% relative humidity, the mole fraction of water vapor is 0.031. If the relative humidity of the atmosphere is zero, Eqn. 23 gives $\delta^{15}N = -0.031 \times 0.0068 = -0.21‰$. This is close to the anomaly of about −0.2‰ observed in the dune.

3.1. Effect of Temperature Gradients on the Isotope Profile

Pronounced seasonal temperature transients propagate downward into the study dune to a depth of about 10 m (Fig. 5). In addition, the data show a strong geothermal gradient of about 0.06°C m^{-1}. We expect these temperature gradients to modulate the isotope profile for two reasons. First, thermal diffusion will occur, forcing the heavier isotopes toward the colder spots (Grew and Ibbs, 1952). Second, the temperature dependence of the saturation vapor pressure causes the mole fraction of water vapor, and hence the water vapor flux fractionation effect, to increase in the warm areas. Both effects conspire with the geotherm to weaken the isotope gradient (i.e., make the profile closer to vertical), whereas the impact of temperature seasonality in the upper 10 m is more complicated. The steady-state analytical model given above is not valid for treating seasonality as the profile is not at steady state on a 6-month timescale.

To assess the impact of seasonality we built a time-dependent numerical model of the water vapor flux fractionation effect that incorporates fractionation due to gravity and thermal diffusion (details of the model architecture are given in Appendix A). The model is forced with a separate thermal model that is constrained by our temperature observations. Like the steady state model, the time-dependent model has only one free parameter, the atmospheric water vapor mole fraction used as a boundary condition.

The dashed lines in Fig. 3 show the results of the time-dependent model with three different atmospheric vapor contents: 0, 1, and 2% (absolute humidity or mole fraction). Notice in Fig. 3 that the model reproduces the observed hook-shaped minimum in $\delta^{15}N$ at 10 m depth and the gradual increase from 10 m depth to the surface, which is not explained by the steady-state model. The minimum at 10 m depth corresponds to a local maximum in temperature (Fig. 5), which is the previous summer's warmth propagating downward. Our interpretation is that thermal diffusion is forcing the light isotopes into the temperature maximum, creating the $\delta^{15}N$ minimum. Support for this view is provided by model runs in which the thermal diffusion effect is isolated from the other effects (Fig. 6). These runs show the hook shape clearly.

For ^{15}N, the best fit atmospheric water vapor content would appear to be about 1% absolute humidity, judging from the dashed curves in Fig. 3. Unfortunately, we have no long-term meteorological data from the dune site, but the weather station at the El Centro Naval Air Station located

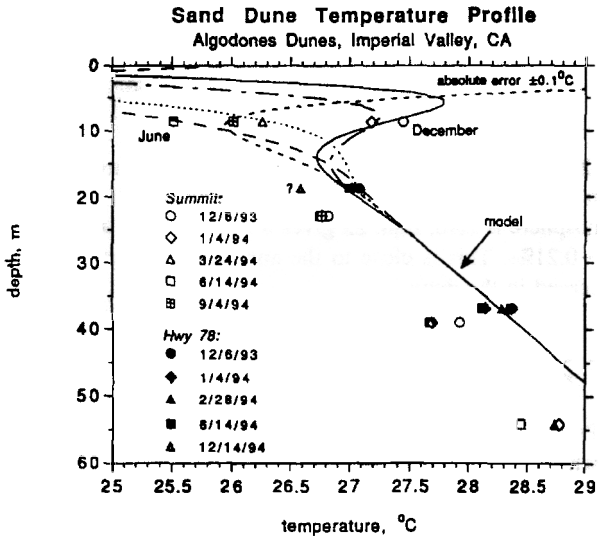

FIG. 5. Temperature in the sampling holes. Four-wire thermisters were buried along with the intake screens, and measured temperatures are shown by the symbols. Note the geothermal gradient below 20 m and the seasonality at 10 m. The lines are snapshots of the temperature model used to drive the numerical isotope model, shown at the times when the temperature observations were made in the Summit hole. Temperature model is described fully in Appendix A.

52 km WSW of the site (Fig. 1) keeps dew point observations. The weather station is in the same climatic zone as the dunes, and the instruments are kept above dry dirt, but the heavy irrigation of the surrounding agricultural fields may make the station humidity an upper limit on the humidity at the dunes. From a 13-year average of monthly mean dew point (National Weather Service, 1995) we calculate a mean annual absolute humidity of 0.84%. Given the uncertainties in the temperature model used to drive the isotope model, this mismatch with the best fit of 1% is probably not significant.

For the ^{18}O data (Fig. 3) there is more scatter but again the 1% absolute humidity fits fairly well. A slight mismatch between the Hwy 78 and Summit holes in both nitrogen and oxygen is expected because the temperature at any given depth is ~0.5°C higher in the Hwy 78 hole than in the Summit hole, and the thermal model was made to match Hwy 78 hole temperatures. Running the model at the lower temperatures of the Summit hole produces a +0.05‰ shift in $\delta^{18}O$ and a +0.03‰ shift in $\delta^{15}N$.

A stringent test of our hypothesis would be to examine the near-surface profiles in the opposite season, that is, in September. We have done this and the results are given in Fig. 7. Note the good match of the seasonal model, which is run for 1% absolute humidity in the atmosphere, with the September nitrogen and oxygen isotopic observations. We infer that the sharp contrast between the two seasons is due primarily to thermal diffusion.

4. LABORATORY SIMULATION OF VAPOR EFFECT

To further test the model reached via diffusion theory, we performed a laboratory simulation of the hypothesized effect. Quartz wool was packed into 9 mm o.d. glass tubing to form diffusive columns 14 cm long, and ~10 μL H_2O (liquid) was placed at the bottom of the columns in a 2 cm^3 reservoir that could be isolated from the columns with a valve using viton O-rings and a glass stem (Fig. 8). Four samples and four blanks were run, the blanks being identical to the samples in all ways other than containing no H_2O. The columns were equilibrated with dry air blown past the tops of the columns for 12 h at room pressure (nominally 1 atm) and 22.5°C in a temperature bath. We believe the effect develops in a time equal to the diffusion time for the distance (22 cm) between the liquid and the dry advective regime, which in this case is about 40 min, so in 12 h we expect a steady state to have been reached.

After equilibration the valves were closed, isolating 2 cm^3 of air whose composition should have been modified if our hypothesis is correct. The quartz wool was removed and the sample container transferred to the mass spectrometer inlet, where it was submerged 37 mm in an isopropyl alcohol bath at −100°C for 30 min to freeze out all H_2O. The sample was expanded into the mass spectrometer inlet for exactly 5 min while still in the alcohol bath, which was monitored for temperature constancy between samples. Samples were run against the dry air used in the equilibration as a reference gas. The mass spectrometer is the above-mentioned MAT 252 with precision as indicated. In addition to the isotopes, the O_2/N_2 ratio was measured via the mass 32 to mass 29 ratio, with precision of $\delta O_2/N_2 = \pm 0.02‰$. After the analysis, the mass of liquid water remaining in the sample volume was determined by weighing, vacuum drying, and reweighing. Raw results of the four samples and four blanks are shown in Fig. 9.

Notice the large depletion in the blanks, as expected from thermal diffusion fractionation during the expansion in a 120°C temperature gradient. This is unfortunate but we know

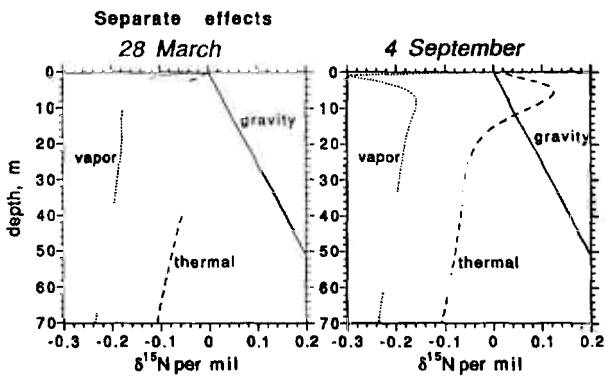

FIG. 6. Separate gravitational, thermal diffusion, and water vapor flux fractionation effects predicted by the seasonal numerical model with 1% atmospheric humidity. A linear combination of the three effects results in the ^{15}N model profile for 1% atmospheric humidity given in Fig. 3. Temperature seasonality affects the shallow part of the profile because of both thermal diffusion and the fact that the water vapor pressure is highly temperature sensitive. Note that the gravitational enrichment with depth is countered by the other two effects because the other two effects increase with depth due to the increase in temperature along the geothermal gradient.

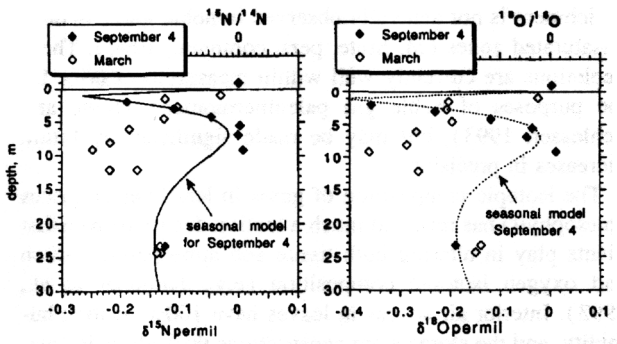

FIG. 7. Near-surface profiles of nitrogen and oxygen isotopes on September 4 with seasonal numerical model run for 1% atmospheric absolute humidity. Note the good fit of the data with the model and the sharp contrast with the March data.

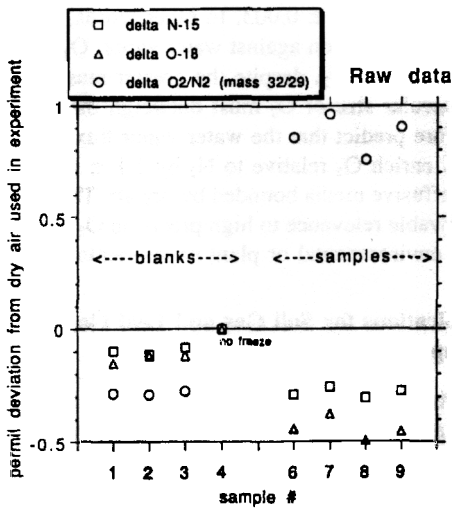

FIG. 9. Raw results of the laboratory simulation. Data is spread arbitrarily along the horizontal axis for visual clarity. To check for sources of noise other than thermal diffusion fractionation we ran one blank without freezing it, the results of which are labeled "no freeze." Blanks gain their identity as such by having no water.

of no better method at present for keeping H_2O out of the mass spectrometer. Since both blanks and samples were treated exactly the same, however, we feel confident in subtracting the means of the three blanks from the samples to obtain our results, shown in Table 2.

One possible source of error in the O_2/N_2 measurement is that freezing the liquid water may have expelled all gases in solution. Since O_2 is twice as soluble as N_2, the addition of these gases to the sample would have introduced bias (this effect is negligible for isotopes because of the much smaller solubility contrasts). Using the measured mass of liquid remaining and the solubilities of Weiss (1970), we calculate that, had all the dissolved gases been expelled, $\delta O_2/N_2$ would have been increased by 0.08‰ and our reported figure in Table 2, 1.15‰, should be reduced to 1.07‰. However, $\delta O_2/N_2$ shows no positive correlation with the amount of liquid, which ranged from 5 to 16 mg, so we suspect that the gases were not expelled, perhaps because freezing occurred too quickly.

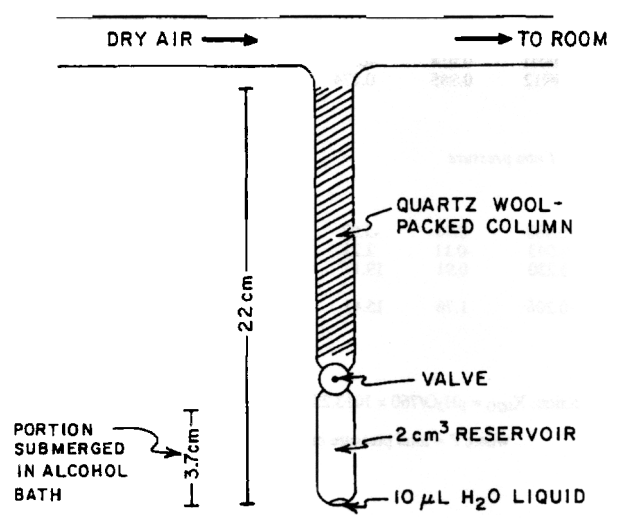

FIG. 8. Schematic diagram of experimental setup used to verify the proposed mechanism. Quartz wool was packed into a tube to prevent advection but permit diffusion. Dry air was blown at ~30 $cm^3 min^{-1}$ past the top of the quartz wool column and vented to the room for 12 h to allow the effect to reach a steady state. Then the valve was closed and the sample admitted to the mass spectrometer while partially submerged in a −100°C bath.

5. DISCUSSION

Agreement with theory appears to be good for the experimental values of $\delta^{15}N$ of N_2 and $\delta^{18}O$ of O_2, but poor for $\delta O_2/N_2$. This is perhaps not surprising because the theory for the relative diffusivities of isotope pairs is robust, depending only on the relative masses, whereas the theory for molecular pairs such as O_2 and N_2 is weaker since molecular volumes and shapes come into play (Reid et al., 1977). Published experimental values of the diffusivities of O_2 and N_2 vary widely and even disagree about which one is faster (e.g., Lide, 1993; Table 11-2 in Reid et al., 1977). The theoretical estimate for $\delta O_2/N_2$ in Table 2 was based on a diffusivity ratio (mass 29/mass 32) of 0.973 obtained via the semiempirical method of Fuller, Schettler, and Giddings as described in Reid et al. (1977).

Assuming that our hypothesis is correct, and taking our experimental result at face value, this ratio should be 0.958 ± 0.003, and the ratio for N_2 and O_2 without isotopic distinc-

Table 2. Results of laboratory simulation of vapor fractionation effect at 22.5°C

	$\delta^{15}N$ of N_2	$\delta^{18}O$ of O_2	$\delta O_2/N_2$ (mass 32/29)
THEORETICAL (uncertainty arises from temperature measurement)	-0.187 ±0.005	-0.289 ±0.005	+0.74 ±0.02
EXPERIMENTAL (mean and std dev of four samples with blank subtracted)	-0.185 ±0.02	-0.31 ±0.05	+1.15 ±0.09

tion should be 0.965 ± 0.003. In other words, we find that with regard to diffusion against water vapor, O_2 is 3.6 ± 0.3 percent faster than N_2, despite the greater mass of O_2. The small molecular size of O_2 must outweigh the mass effect. We therefore predict that the water vapor flux fractionation effect will enrich O_2 relative to N_2 by 1.1 ± 0.1‰ at 25°C in moist diffusive media bounded by dry air. This conclusion has conceivable relevance to high precision O_2 measurement involving environmental or plant experimental systems.

5.1. Implications for Soil Gas and Leaf Gas Composition

Using the semiempirical method of Fuller, Schettler, and Giddings as described in Reid et al. (1977), we provide in Table 3 the calculated diffusivity ratios of a variety of gases and the expected vadose zone gas composition in arid regions due to the three effects identified here. As a caveat we note that our analysis neglects Knudsen diffusion, which may be important in fine-grained soils. Any effect of advection is neglected based on the argument (Severinghaus, 1995) that diffusion is likely to overwhelm advective processes in almost all soils at almost all times, except for very near the surface or in special cases where topography and wind combine to produce windpumping (e.g., Weeks, 1994).

Given a typical geotherm of 0.03°C m^{-1}, a mean annual temperature of 20°C, and a dry atmosphere, xenon will be depleted relative to air by 10‰ near the surface (Fig. 10). This would just cancel the enrichment of xenon due to gravitational fractionation at a depth of 30 m. Thus, the water vapor flux fractionation effect may explain why gravitational enrichment is not generally observed in noble gases in deep unsaturated zones (M. Stute, pers. commun., 1994). These depletions are currently well within measurement error for the purposes of noble gas paleothermometry (Stute and Schlosser, 1993), but may be made significant by future increases in precision.

The isotopic composition of gases in leaf interior spaces (mesophyll) has received much attention due to the role that plants play in altering both tissue and atmospheric carbon and oxygen isotopic composition (e.g., Farquhar et al., 1993). Interior air spaces in leaves have 100% relative humidity, and the stomata are constrictions through which water vapor diffuses, so the gas composition in leaves in arid climates may be altered by the water vapor flux fractionation effect. At 25°C in dry air, $\delta^{18}O$ of O_2 in such a leaf would be offset by −0.34‰, $\delta^{18}O$ of CO_2 by −0.2‰, and $\delta^{13}C$ of CO_2 by −0.1‰ from the values that otherwise would obtain. These are small effects compared to the signals of interest in most all studies, but may become important as techniques are refined.

Finally, a future application of the water vapor flux fractionation effect might involve the development of proxy indicators of humidity and precipitation at times in the past. Because the magnitude of the effect is linear in atmospheric humidity, in principle the isotopic composition of soil gas could be inverted to yield mean absolute humidity (as we did in estimating the figure of 1% for the dune site). Soil gases become dissolved in groundwater, and certain aquifers contain an archive of glacial age groundwater (Stute and Schlosser, 1993). Because the water vapor flux fractionation effect is not strictly mass dependent as we show here, mea-

Table 3. Parameters for calculating gravity, thermal diffusion, and vapor flux fractionation effects on some soil gases

Gas pair	$^{15}N^{14}N$ - $^{14}N_2$*	$^{18}O^{16}O$ - $^{16}O_2$*	^{36}Ar - ^{40}Ar	^{38}Ar - ^{40}Ar	O_2 - N_2*	He - air	Ne - air	Ar - air	Kr - air	Xe - air
Mass of first minus mass of second	1	2	-4	- 2	4	-24.95	-8.95	11.05	55.05	102.05
Thermal diffusion factor of pair	0.0069	0.0107	-0.0147	-0.0071	0.018	-0.36	-0.1	0.07	0.1	0.1
Relative diffusivities with water vapor (second/first)	1.0068	1.0108	0.9832	0.9912	0.965	0.274	0.622	0.985	1.253	1.449
Example: *Mean surface temperature 20°C, geothermal gradient 0.03°C m^{-1}, dry atmosphere, 1 atm pressure*										
Expected permil enrichment of first gas relative to second at 60 m depth (by mole fraction):										
Components:										
Gravitational	0.240	0.480	-0.959	-0.480	0.96	-5.97	-2.15	2.65	13.30	24.79
Thermal diffusion	-0.042	-0.065	0.090	0.043	-0.11	2.21	0.61	-0.43	-0.61	-0.61
Vapor flux fractionation	-0.178	-0.282	0.439	0.230	0.91	19.17	9.94	0.39	-6.60	-11.66
Total	0.019	0.132	-0.430	-0.206	1.76	15.41	8.40	2.61	6.08	12.52

Equations (4), (5), and (22) are used in these calculations, in addition to:

Saturation vapor pressure: pH_2O (mmHg) = $a + bT + cT^2 + dT^3$ Water vapor mole fraction: $X_{H2O} = pH_2O/760 \times 1013.25/P$

where T = temperature in °C
a = 1.69803084
b = 0.7568078
c = - 0.0109724
d = 0.00063967

where P = total pressure in mbar

*neglects biological effects which can be substantial

Sources:
Gravitational fractionation as in Craig et al. (1988).
Thermal diffusion factors from Grew and Ibbs (1952), Thermal diffusion in gases, Cambridge U. Press.
Diffusivities with water vapor calculated using the method of Fuller et al. as given in Reid et al. (1977) except for O_2 - N_2, which was measured experimentally (this paper).

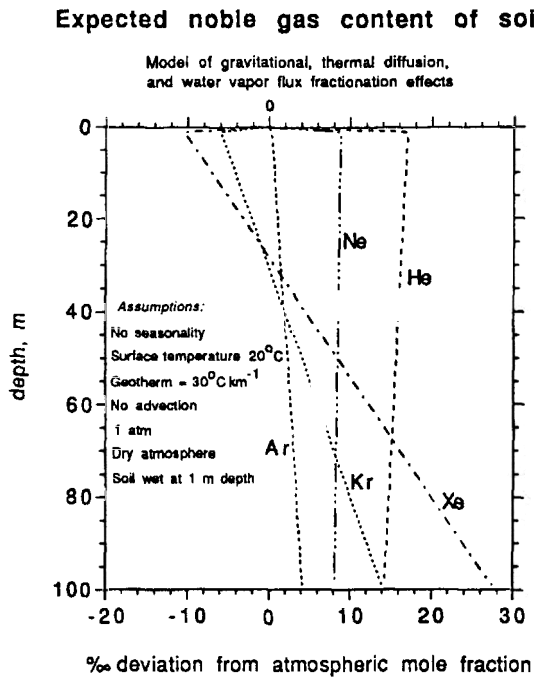

FIG. 10. Predicted soil air noble gas composition based on the three effects discussed in this paper. Anomaly is presented as the permil fractional deviation of the noble gas/air ratio from the atmospheric ratio, for example: $[(Xe/air_{sample})/(Xe/air_{atmosphere}) - 1]10^3‰$. These effects make small contributions to the makeup of the gases dissolved in groundwater, in addition to the major role played by solubility.

suring several isotope pairs simultaneously may allow removal of the gravitational signal. For example, $^{36}Ar/^{40}Ar$ is fractionated four times as much as $^{15}N/^{14}N$ by gravity, yet only twice as much by the water vapor flux fractionation effect (Table 3). A correction for the solubility contrast must also be made. Combined with paleotemperature from noble gas abundance (Stute and Schlosser, 1993) and assumptions about the geothermal gradient, the atmospheric humidity at times in the past is isolated as the only remaining parameter. Paleohumidity is presently one of the least constrained variables in paleoclimate reconstructions, yet it is one of the most important given the postulated role of the hydrological cycle in abrupt climate change (Chappellaz et al., 1993).

6. SUMMARY

Negative isotopic anomalies observed in unsaturated zone O_2 and N_2 from sand dunes can be explained by fractionation due to a diffusive flux of water vapor out of the wet dune into the dry air, a mechanism we name the water vapor flux fractionation effect. Quantitative confirmation of the mechanism is provided by a laboratory simulation of the effect and by a calculation from diffusion theory. Additional fractionation effects arise from thermal diffusion and gravitational settling. We predict that soil gases in general will enjoy these three effects. The water vapor effect will also occur in gas phases in leaves in arid regions, and potentially any moist diffusive environment bounded by an advectively well-mixed dry atmosphere.

Acknowledgments—David Archer suggested the algorithm for the time-dependent model. The manuscript benefitted from reviews by Tetsu Tokunaga and two anonymous reviewers. John Gregg of Gregg Drilling, Signal Hill, Ca., USA, generously donated services to drill the 60-m deep holes. Joe Orchardo helped with the laboratory simulation, and Taylor Ellis did the dune air isotopic analyses. Preliminary mass spectrometric work and the soil water content analyses were done in the laboratory of Martin Wahlen. Bruce Deck's generosity with his time, equipment, and vehicles was crucial for the success of the field work. Bill Paplawski, Derek Mastroianni, Tom Baker, and other students and staff in Martin Wahlen's laboratory provided field assistance. The El Centro Office of the U. S. Bureau of Land Management graciously gave us permission to use the sand dunes, which fall under their jurisdiction. J.P.S. was supported in this work by a Graduate Fellowship for Global Change sponsored by the U. S. Department of Energy and administered by Oak Ridge Institute for Science and Education.

Editorial handling: G. Sposito

REFERENCES

Bender M. L., Sowers T., Barnola J.-M., and Chappellaz J. (1994a) Changes in the O_2/N_2 ratio of the atmosphere during recent decades reflected in the composition of air in the firn at Vostok Station, Antarctica. *Geophys. Res. Lett.* **21,** 189–192.

Bender M. L., Tans P. P., Ellis J. T., Orchardo J., and Habfast K. (1994b) A high precision isotope ratio mass spectrometry method for measuring the O_2/N_2 ratio of air. *Geochim. Cosmochim. Acta* **58,** 4751–4758.

Bird R. B., Stewart W. E., and Lightfoot E. N. (1960) *Transport Phenomena.* Wiley.

Chang J.-H. (1958) *Ground Temperature,* Vol. I. Harvard Univ.

Chapman S. and Cowling T. G. (1970) *The Mathematical Theory of Non-Uniform Gases.* Cambridge Univ. Press.

Chapman S. and Dootson F. W. (1917) Thermal diffusion. *Phil. Mag.* **33,** 248–253.

Chappellaz J., Blunier T., Raynaud D., Barnola J. M., Schwander J., and Stauffer B. (1993) Synchronous changes in atmospheric CH_4 and Greenland climate between 40 and 8 kyr BP. *Nature* **366,** 443–445.

Clements W. E. and Wilkening M. H. (1974) Atmospheric pressure effects on ^{222}Rn transport across the Earth-air interface. *J. Geophys. Res.* **79,** 5025–5029.

Craig H., Horibe Y., and Sowers T. (1988) Gravitational separation of gases and isotopes in polar ice caps. *Science* **242,** 1675–1678.

Cunningham R. E. and Williams R. J. J. (1980) *Diffusion in Gases and Porous Media.* Plenum.

Dalton J. (1826) On the constitution of the atmosphere. *Phil. Trans.,* Part II, 174–187.

Delwiche C. C. and Steyn P. L. (1970) Nitrogen isotope fractionation in soils and microbial reactions. *Environ. Sci. Techn.* **4,** 929–935.

Farquhar G. D. et al. (1993) Vegetation effects on the isotope composition of oxygen in atmospheric CO_2. *Nature* **363,** 439–443.

Gibbs J. W. (1928) *Collected Works, Vol. 1, Thermodynamics.* Yale Univ. Press.

Grew K. E. and Ibbs T. L. (1952) *Thermal Diffusion in Gases.* Cambridge Univ. Press.

Hesterberg R. and Siegenthaler U. (1991) Production and stable isotopic composition of CO_2 in a soil near Bern, Switzerland. *Tellus* **43B,** 197–205.

Kincaid J. M., Cohen E. G. D., and Lopez de Haro M. (1987) The Enskog theory for multicomponent mixtures. IV. Thermal Diffusion. *J. Chem. Phys.* **86,** 963–975.

Lide D. R. (1993) *Handbook of Chemistry and Physics.* CRC Press.

Mazor E. (1972) Paleotemperatures and other hydrological parame-

ters deduced from noble gases dissolved in groundwaters, Jordan Rift Valley Israel. *Geochim. Cosmochim. Acta* **36,** 1321–1336.
National Weather Service (1995) Climatological Center, Desert Research Institute, University of Nevada, Reno, Nevada.
Reid R. C., Prausnitz J. M., and Sherwood T. K. (1977) *The Properties of Gases and Liquids,* 3rd ed. McGraw-Hill.
Schleser G. H. (1979) Oxygen isotope fractionation during respiration for different temperatures of *T. utilis* and *E. coli* K12. *Radiation and Environmental Biophysics* **17,** 85–93.
Schwander J., Barnola J.-M., Andrie C., Leuenberger M., Ludin A., Raynaud D., and Stauffer B. (1993) The age of the air in the firn and the ice at Summit, Greenland. *J. Geophys. Res.* **98,** 2831–2838.
Severinghaus J. P. (1995) Studies of the terrestrial O_2 and carbon cycles in sand dune gases and in Biosphere 2. Ph.D. dissertation, Columbia Univ.
Sowers T., Bender M., and Raynaud D. (1989) Elemental and isotopic composition of occluded O_2 and N_2 in polar ice. *J. Geophys. Res.* **94,** 5137–5150.
Stute M. and Schlosser P. (1993) Principles and applications of the noble gas paleothermometer. In *Climate Change in Continental Isotopic Records* (ed. P. K. Swart et al.); *Geophys. Monogr. 78,* pp. 89–100. Amer. Geophys. Union.
Stute M., Schlosser P., Clark J. F., and Broecker W. S. (1992) Paleotemperatures in the southwestern United States derived from noble gases in groundwater. *Science* **256,** 1000–1003.
Sweet M. L., Kocurek G., and Havholm K. (1991) A Field Guide to the Algodones Dunes of Southeastern California. In *Geological Excursion in Southern California and Mexico* (ed. M. J. Walawender and B. B. Hanan); Guidebook, 1991 Annual Meeting of the Geological Society of America, pp. 171–185.
Thorstenson D. C. and Pollock D. W. (1989) Gas transport in unsaturated zones: Multicomponent systems and the adequacy of Fick's Laws. *Water Resources Res.* **25,** 477–507.
USGS (1976) Selected Data on Water Wells, Geothermal Wells, and Oil Tests in Imperial Valley, California. U.S. Geological Survey Open-File Report.
Weeks E. P. (1994) Thermal and wind pumping as mechanisms for passive vapor extraction in hilly terrain. *Eos* **75,** 263 (abstr.).
Weiss R. F. (1970) The solubility of nitrogen, oxygen, and argon in water and seawater. *Deep-Sea Res.* **17,** 721–735.

APPENDIX A

Time-Dependent Numerical Model of Water Vapor Flux Fractionation Effect

Model architecture

The algorithm for the water vapor flux fractionation effect is essentially a finite-difference advection-diffusion scheme with the constraint that pressure remain constant. It works by assuming that the gradient in N_2 forces a diffusive flux into the dune, which in turn forces an advective flux out of the dune to maintain constant pressure. As explained in the introduction, this interpretation is not strictly correct because the diffusive fluxes calculated thusly are valid in the no-net-flux reference frame, which is not stationary with respect to the dune. However, as shown below, the model reproduces the analytical solution correctly when run to a steady state, so this approximation appears to be acceptable.

The column of gas is divided up into 100 boxes 1 m deep each. Three gases are modeled, gas i, gas j, and H_2O, where the result is expressed in δ_i. Any effect of other gases present is neglected. Diffusive fluxes of each gas species into a given box are first calculated based on the gradients with neighboring boxes, and then the advective velocity required to satisfy the pressure constraint is calculated. Finally, the actual fluxes are calculated as the sum of diffusive and advective terms, the advective terms being the product of the calculated advective velocity and the upstream concentrations. Figure A1 shows this in schematic form.

Diffusive fluxes are calculated from the difference between the concentration gradient and the thermal/gravitational equilibrium

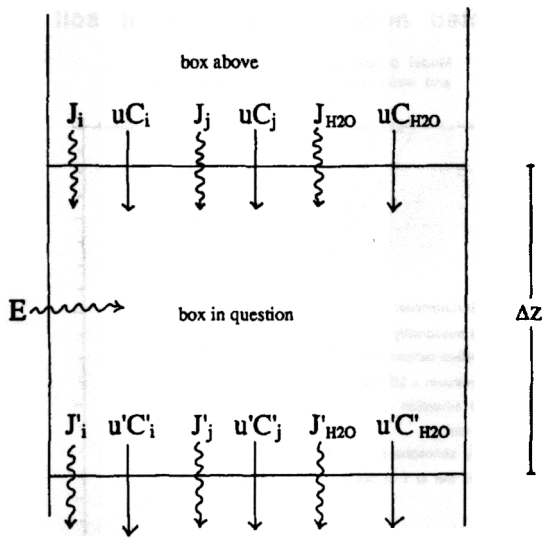

FIG. A1. Diagram of the fluxes considered in the model with their symbols. All vector quantities are positive downwards. Serpentine arrows are diffusive fluxes; straight arrows are advective fluxes. E is evaporation of H_2O (or condensation if negative).

concentration gradient, in effect "relaxing" the concentrations back to the equilibrium profile at the rate given by the diffusivity. Justification for this approach is discussed by Bender et al. (1994a). We note also that thermal diffusion proceeds at the speed of ordinary diffusion (Chapman and Dootson, 1917). Diffusive fluxes J are given in principle by the equation

$$J = -D(d[C - C_{eq}]/dz) \quad \text{(Bender et al., 1994a)}, \quad \text{(A1)}$$

where D is the diffusivity, C is concentration in mol m^{-3}, C_{eq} is the thermal/gravitational equilibrium concentration, and dz is a depth increment. The gradient dC/dz is calculated by difference with the neighboring box above in a finite difference approximation, yielding

$$J_i = -D_i[C_i - C_{io} \exp(mg\Delta z/R^*T_o) - (C_{io} + C_{jo})/\{[T_o/T]^{\alpha}C_{jo}/C_{io} - C_{io}\}]/\Delta z, \quad \text{(A2)}$$

$$J_j = -D_j[C_j - C_{jo} \exp(mg\Delta z/R^*T_o) - (C_{io} + C_{jo})/\{[T_o/T]^{-\alpha}C_{io}/C_{jo} - C_{jo}\}]/\Delta z, \quad \text{(A3)}$$

where J_i = diffusive flux of gas i into the top of a box; C_i = concentration of gas i in the box in question; C_{io} = concentration of gas i in the box above; T = temperature in the box in question, K; T_o = temperature in the box above, K; and α = thermal diffusion factor $i - j$, for calculating δ_i. Note: $\alpha_{i-j} = -\alpha_{j-i}$ ($\alpha_{N15-N14} = 0.006$, $\alpha_{O18-O16} = 0.0107$; Grew and Ibbs, 1952); m = molecular weight; g = acceleration of gravity; Δz = box size; R^* = gas constant; and where the diffusivities are functions of gas type, temperature, and pressure

$$D_i = \tau D_{298,\,1\,atm}[T_o/298.15]^{1.75}/P \quad \text{(Reid et al., 1977)}, \quad \text{(A4)}$$

where $D_{298,\,1\,atm}$ is the free air diffusivity at 298.15 K, 1 atm, τ is a tortuosity factor taken to be 0.6 for this sand dune (Severinghaus, 1995), and P is pressure in atm.

The major gas diffusivity D_j is the binary diffusivity against $^{14}N_2$ (the self-diffusivity D_{j-j} in the case where the major gas is $^{14}N_2$), while for the isotope pair being modeled for the vapor flux effect (like $^{15}N^{14}N$) the diffusivity D_i is the major gas diffusivity times the ratio of the binary diffusivities against water vapor of the two species:

$$D_j = D_{j-N14}, \quad \text{(A5)}$$

$$D_i = D_{j\text{-}N_{14}} D_{i\text{-}H_2O} / D_{j\text{-}H_2O}. \quad \text{(A6)}$$

This way both the water vapor flux fractionation effect and the bulk transport of the thermal diffusion isotopic signal come out approximately correctly. This model uses $D_{N14\text{-}N14} = 0.198$, $D_{O16\text{-}N14} = 0.1997$, and $D_{H_2O\text{-}N14} = 0.274$ cm^2 s^{-1} at 298.15 K, 1 atm (Reid et al., 1977).

The model is for three gases only, and neglects the dependence of α on the presence of other gases in abundance.

Advection velocity u at the top boundary of each box is calculated in the following way. Advective flux is given by uC. All fluxes must sum to zero during each time step, in other words, we impose the constraint that pressure be constant:

$$J_i + J_j + J_{H_2O} + uC_i + uC_j + uC_{H_2O} - J_i' - J_j' - J_{H_2O}' - u'C_i' - u'C_j' - u'C_{H_2O}' + \Delta zE = 0, \quad \text{(A7)}$$

where E is evaporation of H_2O (E may be negative), and the $'$ indicates the bottom of the box. All terms in this equation have units of mol m^{-2} d^{-1}. Next we invoke conservation of H_2O:

$$\Delta zE + J_{H_2O} + uC_{H_2O} - J_{H_2O}' - u'C_{H_2O}' = \Delta z dC_{H_2O}/dt. \quad \text{(A8)}$$

Subtracting Eqn. A8 from A7 and solving for u, we get

$$u = (u'(C_i' + C_j') + J_i' + J_j' - J_i - J_j - \Delta z dC_{H_2O}/dt)/(C_i + C_j). \quad \text{(A9)}$$

The only unknowns on the right-hand side of Eqn. A9 are u' and dC_{H_2O}/dt. The time derivative dC_{H_2O}/dt is calculated by difference with the previous time step. C_{H_2O} is calculated from the saturation vapor pressure curve and the temperature given by the independent temperature model (assuming 100% relative humidity in the box in all portions of the model where liquid water coats the grains).

Time derivatives for other gases are calculated according to

$$dC/dt = [J + uC_{up} - J' - u'C_{up}']/\Delta z, \quad \text{(A10)}$$

where C_{up} is the upstream concentration determined as follows: if $u > 0$, then $C_{up} = C_0$, if $u \leq 0$, then $C_{up} = C$.

Calculation is started at the deepest box, at the water table, which represents a no-flux boundary condition (diffusivities in liquid water are orders of magnitude slower than in gases; Reid et al., 1977). In this deepest box, J' and u' are set to zero, enabling calculation of u. The model then works its way upwards through the column, with u and J becoming the u' and J' of the next box up. When the model reaches the wetting front a different algorithm is used, since liquid water is no longer present. E is set to zero and Eqn. A7 alone is used to solve for u, with J_{H_2O} calculated explicitly from Eqn. A1 and C_{H_2O} from Eqn. A10. The position of the wetting front is imposed and constant (1 m depth for this model). Atmospheric concentrations including water vapor are imposed and held constant, forming the top boundary condition. After all time derivatives are calculated, the model concentrations are advanced one time step Δt (=0.2 days for this model):

$$C = C + dC/dt\Delta t. \quad \text{(A11)}$$

The model is run for 100 years to allow it to reach a steady state. With $D \approx 1$ m^{2}d^{-1}, depth of interest $h = 60$ m, the diffusion time $\tau = h^2/D = 3600$ d, so 100 years is about 10 diffusion times.

Temperature Model

We force the isotope model with a thermal model that essentially serves to interpolate between the temperature data points, which are rather sparse. The thermal model has a constant thermal diffusivity of 0.14 m^2 d^{-1}, which was obtained by fitting the 5 observations at 8.23 m depth and one observation at the surface (Fig. A2), together with the mean annual surface temperature of 25.8°C obtained by upward linear extrapolation of the observed geothermal gradient in the Hwy 78 hole (Fig. 5). The temperatures in the Summit hole are somewhat lower and extrapolate to a surface value of 25.3°C. These were not used as the Summit hole is on a hill, which causes the heat flow vectors to diverge, reducing the thermal gradient under the hill and invalidating the one-dimensional assumption made in the models. The surface forcing is given by

$$T = 25.8 + 8 \sin(2\pi t - 0.7 \cos(2\pi t)) + 2.632, \quad \text{(A12)}$$

where T is temperature in °C; t is time in years after May 24; 25.8 is the mean surface temperature; 8 is the amplitude of seasonal forcing; and 2.632 compensates for the reduction of the mean due to the cosine term (whose purpose is to make the summers more "peaked"). In addition, the geothermal gradient is given by a bot-

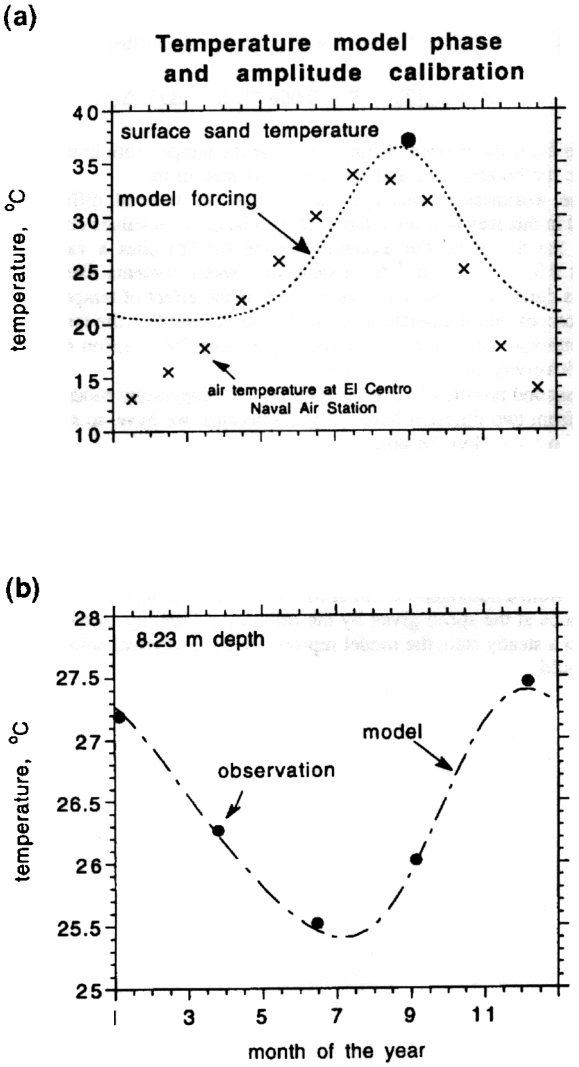

FIG. A2. Temperature observations used to constrain the thermal model. Month 1 is January 1. Notice the change in scale between the upper and lower figures. (a) Surface sand temperature. The single observation shown (●) is the surface intercept of a depth profile of the top 1 m consisting of several dozen measurements during day and night. Monthly mean air temperature at El Centro (×) is shown for comparison (midpoint of average maximum and minimum air temperature over a 13-year period) (National Weather Service, 1995). (b) Temperature at 8.23 m depth. The 8.23 m data along with the mean surface temperature and the single surface observation were used to establish the forcing amplitude, shape, and phase and the thermal diffusivity, by a trial-and-error fit.

tom boundary condition (at the water table) that relaxes the gradient toward +0.0667°C m^{-1} at the speed given by the diffusivity:

$$dT/dt = D_{th}[T_o - T + 0.0667°C\ m^{-1}\ \Delta z]/\Delta z^2, \quad (A13)$$

where D_{th} is the thermal diffusivity, T_o is the temperature in the box above the bottom box, and Δz is the box size in m.

One weakness of this approach is that the thermal diffusivity found in this way is about a factor of 2–3 larger than values obtained from the literature. For example, Chang (1958) cites a value of about 0.03–0.05 $m^2\ d^{-1}$ for a sand with water contents like those in this dune. However, our concern here is the effect of temperature on isotopes, not temperature per se, so we assume that the temperature measurements are correct and leave aside the question of why the diffusivity appears anomalous.

A second problem is that we have fit the temperature model with data from two different holes (Fig. 5) because we have no shallow data from the Hwy 78 hole.

Tests of the Model

Figure A3 shows the initiation of the water vapor flux fractionation effect from a homogenous initial condition, confirming that the effect develops at the speed given by the ordinary diffusivity. Also, when run to a steady state the model reproduces the analytical solution as it should.

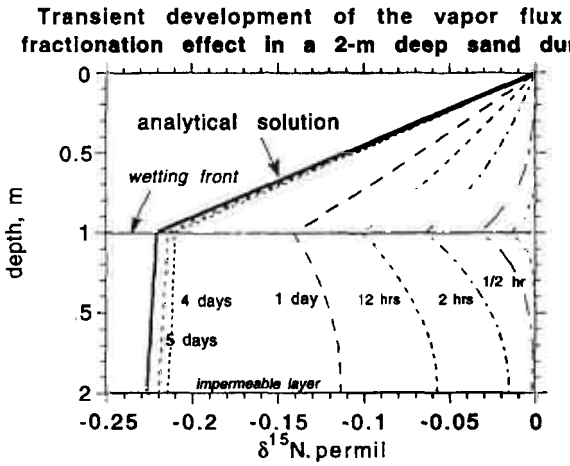

FIG. A3. Transient evolution of the vapor flux fractionation effect from an initially homogeneous state in a hypothetical 2-m deep dune in which the sand is wet at a depth of 1 m. Notice how the effect is concentrated at the wetting front in the early stages. This may explain the sharp depletion at the wetting front during the summer (Fig. 6), when the sand is heating up rapidly causing the vapor mole fraction to increase rapidly.